Geophysical Research Letters

RESEARCH LETTER
10.1029/2021GL093675

Key Points:

- The large-scale spatial structure of sea-level variability along the North American East Coast is time-dependent and frequency-dependent
- Multidecadal epochs of enhanced (up to ~10 cm) decadal sea-level variability are evident at most east coast tide gauges
- From approximately 1960 to 1990, decadal sea-level variability was coherent across Cape Hatteras

Supporting Information:

Supporting Information may be found in the online version of this article.

Correspondence to:

C. M. Little,
clittle@aer.com

Citation:

Little, C. M., Piecuch, C. G., & Ponte, R. M. (2021). North American east coast sea level exhibits high power and spatiotemporal complexity on decadal timescales. *Geophysical Research Letters*, *48*, e2021GL093675. https://doi.org/10.1029/2021GL093675

Received 8 APR 2021
Accepted 28 JUN 2021

North American East Coast Sea Level Exhibits High Power and Spatiotemporal Complexity on Decadal Timescales

Christopher M. Little[1], Christopher G. Piecuch[2], and Rui M. Ponte[1]

[1]Atmospheric and Environmental Research, Inc., Lexington, MA, USA, [2]Department of Physical Oceanography, Woods Hole Oceanographic Institution, Falmouth, MA, USA

Abstract Tide gauges provide a rich, long-term, record of the amplitude and spatiotemporal structure of interannual to multidecadal coastal sea-level variability, including that related to North American east coast sea level "hotspots." Here, using wavelet analyses, we find evidence for multidecadal epochs of enhanced decadal (10–15 year period) sea-level variability at almost all long (>70 years) east coast tide gauge records. Within this frequency band, large-scale spatial covariance is time-dependent; notably, coastal sectors north and south of Cape Hatteras exhibit multidecadal epochs of coherence (~1960–1990) and incoherence (~1990-present). Results suggest that previous interpretations of along coast covariance, and its underlying physical drivers, are clouded by time-dependence and frequency-dependence. Although further work is required to clarify the mechanisms driving sea-level variability in this frequency band, we highlight potential associations with the North Atlantic sea surface temperature tripole and Atlantic Multidecadal Variability.

Plain Language Summary The prediction of future sea-level change along the densely populated North American east coast is of considerable societal value. However, robust predictions require additional efforts to (a) characterize the nature of observed sea-level variability; and (b) identify key underlying physical processes. Such efforts are also required to understand whether, and how, the tide gauge record can be used to reconstruct ocean circulation and climate variability. While many studies have investigated North American east coast sea-level variability, there remains a lack of clarity in its spatial structure. Of particular importance to reconstructions and tide gauge indices is the degree to which sea-level variability is common ('"coherent") across Cape Hatteras. Here, we identify and characterize sea-level variability across a large set of tide gauge records, highlighting changes occurring at roughly decadal periods. Coastal sea level exhibits damped and enhanced 30-40-year epochs of decadal variability, and coherence (~1960–1990), and incoherence (~1990-present) across Cape Hatteras. These findings (a) reveal limitations in assumptions embedded in previous coastal sea-level indices and sea-level reconstructions and (b) inform interpretations of geographic shifts in sea level "hotspots" observed over the past few decades.

1. Introduction

Interannual to multidecadal fluctuations in sea level often overwhelm long-term secular trends, driving changes in the frequency and severity of coastal flooding, salt water intrusion, and coastal erosion events, with important consequences for coastal communities (e.g., Ezer & Atkinson, 2014; Hamlington et al., 2015; Menéndez & Woodworth, 2010; Nicholls & Cazenave, 2010; Sweet et al., 2016). Along the eastern North American coastline (east coast; Figure 1a), rates of sea-level rise have varied widely in time and space over the past two decades, with regions of enhanced rise described as "hotspots" (Sallenger et al., 2012). For example, from 2010 to 2015, the east coast south of Cape Hatteras experienced rates of sea-level rise of up to three times the global mean (Domingues et al., 2018; Valle-Levinson et al., 2017). In contrast, in the previous decade, sea-level rise rates were relatively high north of Cape Hatteras (e.g., Boon, 2012; Kopp, 2013; Sallenger et al., 2012; Yin & Goddard, 2013).

The east coast tide gauge record, extending into the 19th century, provides a valuable means to place recent observations into context. For example, long records can inform whether (a) there are periodic and/or potentially predictable aspects of sea-level variability; and (b) sea-level rates are out-of-phase across the Gulf

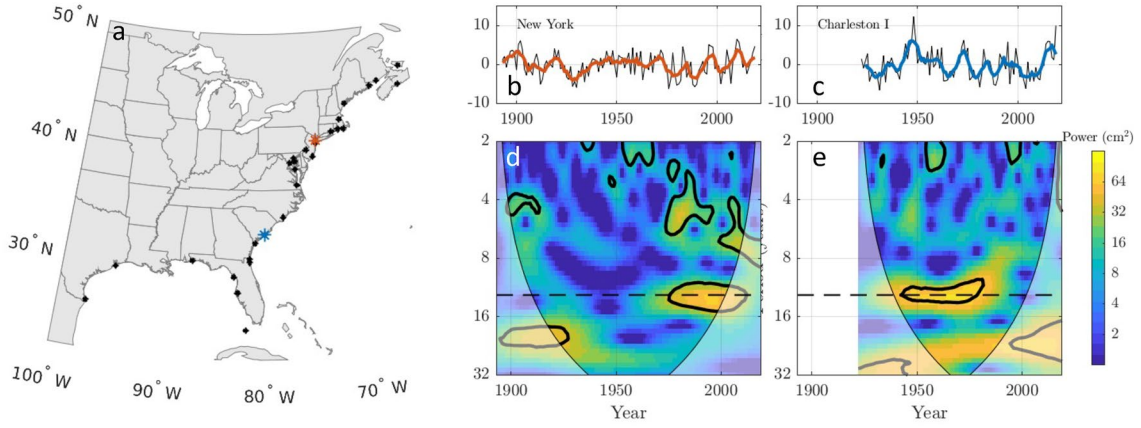

Figure 1. (a) Location of tide gauges employed in this analysis, with colors indicating the two tide gauges highlighted in this figure (Charleston I, blue; the Battery/New York City, orange). (b) Detrended, infilled, annual mean sea level (ζ, in cm) at the Battery tide gauge. (c) as (b), for the Charleston tide gauge. 5-year smoothed time series at each tide gauge are shown with thick colored lines. (d) Continuous wavelet power spectra (in cm^2, on a $\log_2$ scale) of ζ at the Battery tide gauge. Transparent mask indicates the cone of influence. Solid black lines denote significance at the $p < 0.1$ level relative to 300 resampled time series with the same AR(1) coefficients. Black dashed line indicates a period of 12.4 years. (e) As (d), for the Charleston tide gauge (other east coast tide gauges are shown in Figures S3–S5).

Stream detachment at Cape Hatteras, or merely unrelated. Such kinematic information may also inform dynamical considerations, for example, whether hotspots are driven by the same physical process on both sides of Cape Hatteras. An improved understanding of the spatial structure of sea-level variability is also required for assessing the robustness of (a) covariance assumptions embedded in sea-level reconstructions (Kopp, 2013; Piecuch, Huybers, et al., 2018) and (b) tide-gauge based indices of climate variability (e.g., Ezer, 2015; McCarthy et al., 2015; Valle-Levinson et al., 2017).

Previous analyses of east coast sea-level variability generally consider the forcing and dynamics of sea level in sectors north and south of Cape Hatteras separately, often reducing noise by averaging tide gauge records over each along coast sector (e.g., Goddard et al., 2015; Kenigson et al., 2018; McCarthy et al., 2015; Meade & Emery, 1971; Piecuch, Bittermann, et al., 2018; Thompson & Mitchum, 2014). Justification for this approach is generally based on cross-correlation analyses, which reveal higher correlations for tide gauges on the same side of Cape Hatteras than those on opposite sides (Ezer, 2019; Kenigson et al., 2018; McCarthy et al., 2015; Piecuch et al., 2017; Thompson & Mitchum, 2014; Woodworth et al., 2014). However, correlations across Cape Hatteras vary widely across these studies, possibly due to the different time periods and tide gauges considered.

Perhaps relatedly, the along coast extent of sectors also varies across studies. For example, north of Hatteras sectors have included (Piecuch et al., 2017; Thompson & Mitchum, 2014) or excluded (McCarthy et al., 2015; Meade & Emery, 1971) tide gauges in the Gulf of Maine, while the sector south of Cape Hatteras has been chosen to extend to Miami Beach (McCarthy et al., 2015; Thompson & Mitchum, 2014) or Fernandina Beach, excluding much of Florida's Atlantic coast (Kenigson et al., 2018). Kenigson et al. (2018) identify Chesapeake Bay as a distinct sector, whereas other studies often exclude tide gauges within estuaries, bays, and harbors in favor of open-ocean sites (e.g., Thompson & Mitchum, 2014). While it is reasonable that sector definitions should change depending upon the physical process considered (e.g., the North Atlantic Oscillation [NAO], local or remote wind stress, river discharge), most studies do not clearly state the dynamical rationale underlying these choices.

Furthermore, a few studies find evidence for common sea-level variability across Cape Hatteras (Thompson, 1986; Thompson & Mitchum, 2014). In particular, Thompson (1986) notes a frequency-dependent relationship between tide gauges in Charleston and Boston between 1950 and 1975, with significant coherence at periods longer than 6 years. More recent literature has not pursued similar coherence analyses, even with the opportunity to analyze a substantially longer time series. Several recent studies have also suggested that the ocean's response to atmospheric forcing related to the NAO or other large-scale climate modes may result in a coherent, but out-of-phase, relationship between tide gauges north and south of Cape Hatteras

(Kopp, 2013; McCarthy et al., 2015; Valle-Levinson et al., 2017). (The interpretation of south/north differences as a dynamical signal has, however, been challenged (Woodworth et al., 2017); higher correlations between these sea-level indices and climate indices could result from the elimination of common, unrelated sea-level variability.)

Valle-Levinson et al. (2017) employ a more objective approach to assessing east coast sea level covariance in the long-term record. By applying an empirical orthogonal function (EOF) analysis to smoothed rates of sea-level change, this study finds two dominant modes: a dipole across Cape Hatteras (explaining 20% of the variance) and a uniform along coast mode (explaining 67%). However, their EOF-based approach assumes that spatial and temporal dependencies are separable, and thus cannot account for time-dependence and/or frequency-dependence in the spatial structure of sea-level variability. In fact, the decomposition of variance into two modes obscures the strong decadal periodicity, and its apparent amplitude modulation, evident in the tide gauge record (e.g., their Figure 3). Such periods of amplified decadal variability are also clearly evident in time series of long east coast tide gauge records, especially north of Cape Hatteras after ~1960 (e.g., McCarthy et al., 2015; Piecuch et al., 2017; Talke et al., 2018), although they have not been explicitly discussed in the literature.

To summarize, interannual to multidecadal fluctuations in east coast sea level are of critical importance to coastal communities and the interpretation of past ocean circulation, but their spatiotemporal structure is currently poorly characterized. Here, to improve the basis for the identification of underlying driving mechanisms, and their potential predictability, we quantify (a) the time-dependent amplitude of coastal sea-level variability along the east coast, focusing on decadal periods; and (b) the degree to which this variability is spatially coherent, and the epochs of coherence, especially across Cape Hatteras.

2. Data and Methods

We analyze 29 monthly mean tide-gauge records, retrieved from the Permanent Service for Mean Sea Level Revised Local Reference (PSMSL RLR) database on July 1 2020 (Holgate et al., 2013). Tide gauges are included if they include at least 840 monthly mean values over the 1893–2019 period (Figure 1a and Table 1). Monthly values for all tide gauges, relative to 2019, are shown in Figure S1. The Fernandina Beach, Eastport, Halifax, and Charlottetown tide gauge records have been truncated due to extensive gaps early in their record.

East coast tide gauges exhibit long-term increases in relative sea level, with contributions from various local, regional, and global processes, including land motion (e.g., Piecuch, Huybers, et al., 2018). As this analysis focuses on sea-level fluctuations related to climate variability, we linearly detrend the monthly records over the period of record of each tide gauge. After removing the trend, gaps in monthly records are filled by zeros before calculating annual means (Figure S2). Given our focus on decadal signals, our results are insensitive to the details of the gap-filling algorithm. All subsequent analyses are performed on detrended annual mean values (subsequently denoted as ζ).

Wavelet analysis was performed using publicly available MATLAB code (Grinsted et al., 2004) building on work by Torrence and Webster (1999). We use a complex Morlet wavelet with $\omega_0 = 6$ and 61 scales representing Fourier periods from 1.03 to 33 years; results are insensitive to reasonable alternative parameter choices. The "cone of influence" of each tide gauge is a function of the record length (Figures S3–S5).

Uncertainty is assessed using Monte-Carlo techniques. For each tide gauge, we generate 300 synthetic red noise time series of the same length and with identical lag-1 autocorrelation coefficients. Values are considered significant if they are greater than the 90th percentile value of the synthetic time series. Past studies (e.g., Piecuch, Huybers, et al., 2018; Piecuch et al., 2017) show that an autoregressive model of order 1 is a reasonable null model for annual mean tide-gauge records in this region.

Table 1
Tide Gauges Included in This Analysis

Tide gauge	Latitude	Longitude	First full year	Last full year	Completeness
Charlottetown	46.23	−63.12	1938	2018	95.0%
Halifax	44.67	−63.58	1941	2013	96.5%
Saint John, N.B.	45.27	−66.07	1941	2018	89.1%
Eastport	44.9	−66.98	1930	2019	93.8%
Portland (Maine)	43.66	−70.25	1912	2019	99.8%
Boston	42.35	−71.05	1921	2019	99.1%
Woods Hole (Ocean. Inst.)	41.52	−70.67	1933	2019	94.8%
Newport	41.51	−71.33	1931	2019	99.0%
New London	41.36	−72.09	1939	2019	96.5%
New York (The Battery)	40.7	−74.01	1893	2019	99.3%
Sandy Hook	40.47	−74.01	1933	2019	98.8%
Philadelphia (Pier 9N)	39.93	−75.14	1901	2019	97.5%
Atlantic City	39.35	−74.42	1912	2019	93.3%
Baltimore	39.27	−76.58	1903	2019	99.8%
Annapolis (Naval Academy)	38.98	−76.48	1929	2019	96.3%
Washington DC	38.87	−77.02	1931	2019	98.3%
Solomon's Island (Biol. Lab.)	38.32	−76.45	1938	2019	96.2%
Sewells Point, Hampton Roads	36.95	−76.33	1928	2019	99.8%
Wilmington	34.23	−77.95	1936	2019	98.5%
Charleston I	32.78	−79.92	1922	2019	100.0%
Fort Pulaski	32.03	−80.9	1935	2019	98.8%
Fernandina Beach	30.67	−81.47	1939	2019	96.8%
Mayport	30.39	−81.43	1929	1999	99.8%
Key West	24.55	−81.81	1913	2019	99.2%
St. Petersburg	27.76	−82.63	1947	2019	99.9%
Cedar Key II	29.14	−83.03	1939	2019	95.2%
Pensacola	30.4	−87.21	1924	2019	98.6%
Galveston II, Pier 21, TX	29.31	−94.79	1909	2019	99.5%
Port Isabel	26.06	−97.22	1945	2019	96.4%

Note. Completeness is the fraction of months with data over the time period beginning in the first full year and ending in the last full year, inclusive.

3. Results

East coast tide gauges exhibit variability in ζ at a wide range of timescales. When smoothed over interannual frequencies, most reveal substantial longer-period variability. For example, in Figure 1b, ζ at the Battery tide gauge (New York City) shows a shift to more pronounced quasi-decadal variability around 1960–1970. This shift is particularly evident in tide gauges north of Cape Hatteras, and is apparent in earlier studies utilizing long east coast tide gauge records (e.g., Ezer & Dangendorf, 2020; Piecuch et al., 2017; Woodworth et al., 2017). However, epochs of amplified and damped quasi-decadal variability are evident in most tide gauge records along the east coast (Figures 1c and S2).

We employ continuous wavelet transforms to more rigorously investigate the frequency-dependence and time-dependence of ζ variability. Immediately apparent in wavelet spectra for almost all east coast tide gauges (Figures S3–S5) is a band of enhanced power at 10–15 year periods (hereafter, the "decadal" band). Representative spectra at Charleston and New York City are shown in Figures 1d and 1e. While there is

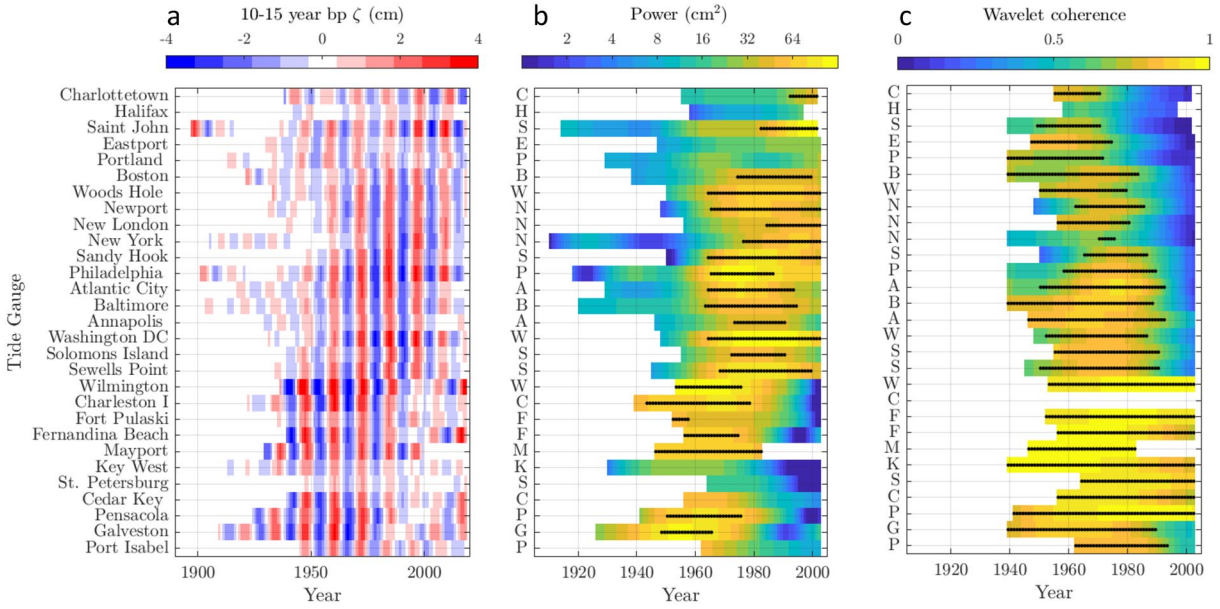

Figure 2. (a) 10–15 years bandpass filtered ζ (in cm) at all tide gauges. (b) Power centered on a period of 12.4 years (in cm^2) for all tide gauges, only shown for times outside the cone of influence. (c) Wavelet coherence of east coast tide gauges with the Charleston I tide gauge centered on a period of 12.4 years. In (b) and (c), significance at the $p < 0.1$ level is shown with stippling.

power at other periods at particular locations (e.g., 5-year and 20-year periods at New York City; Figure 1e), no bands are as consistently prominent and/or significant (see Section 2) as the decadal band. Power in this band is not constant over the period of record, however: ζ exhibits multidecadal epochs of enhanced variability that differ in time along the coast (~1940–1980 and ~1970–2000 at Charleston and the Battery, respectively).

The amplitude of 10–15 year band-pass filtered ζ (Figure 2a) varies over the period of record at all east coast tide gauges. Wavelet power centered on a Fourier period of 12.4 years varies in time and space by over an order of magnitude, consistent with band-passed time series (Figure 2b). While site-to-site differences are evident, epochs of enhanced decadal variability exhibit a distinct spatial structure at a sectoral scale. For example, although there are fewer and shorter tide gauge records available south of Cape Hatteras, the epoch of enhanced power at decadal periods precedes that in tide gauges north of Cape Hatteras. The initiation of significantly enhanced power appears as early as mid-1940s in Charleston and other tide gauges in the Gulf of Mexico. In contrast, most tide gauges north of Cape Hatteras show significant power only after 1965. In the two northernmost tide gauges, significant power emerges only after 1985. During epochs of enhanced ζ variability, maxima in power are similar in magnitude along the east coast (generally between 50 and 100 cm^2). However, these maxima are much lower in some tide gauges, notably Key West and Pensacola, on Florida's west coast, and those along the coast of Maine.

The along coast coherence of ζ variability in the decadal band also varies over multidecadal timescales. In Figure 2c, this behavior is illustrated by calculating wavelet coherence between the Charleston tide gauge and all other east coast tide gauges centered on a period of 12.4 years. While decadal ζ variability from Pensacola to Wilmington is highly coherent with Charleston over the common period of record, tide gauges to the north and west exhibit periods of high and low coherence. For example, the Galveston and Port Isabel tide gauges lose coherence with ζ at Charleston in the 1990s. A similar loss of coherence is evident in tide gauges immediately north of Cape Hatteras, while those north of New York City lose coherence earlier (~1970). Summarizing, over the period of record, power in decadal east coast ζ exhibits a northward shift. As variability becomes weaker south of Cape Hatteras around ~1980, along coast coherence across Cape Hatteras decreases, but remains high for locations north of Cape Hatteras. During times of coherence, ζ variability is largely in-phase.

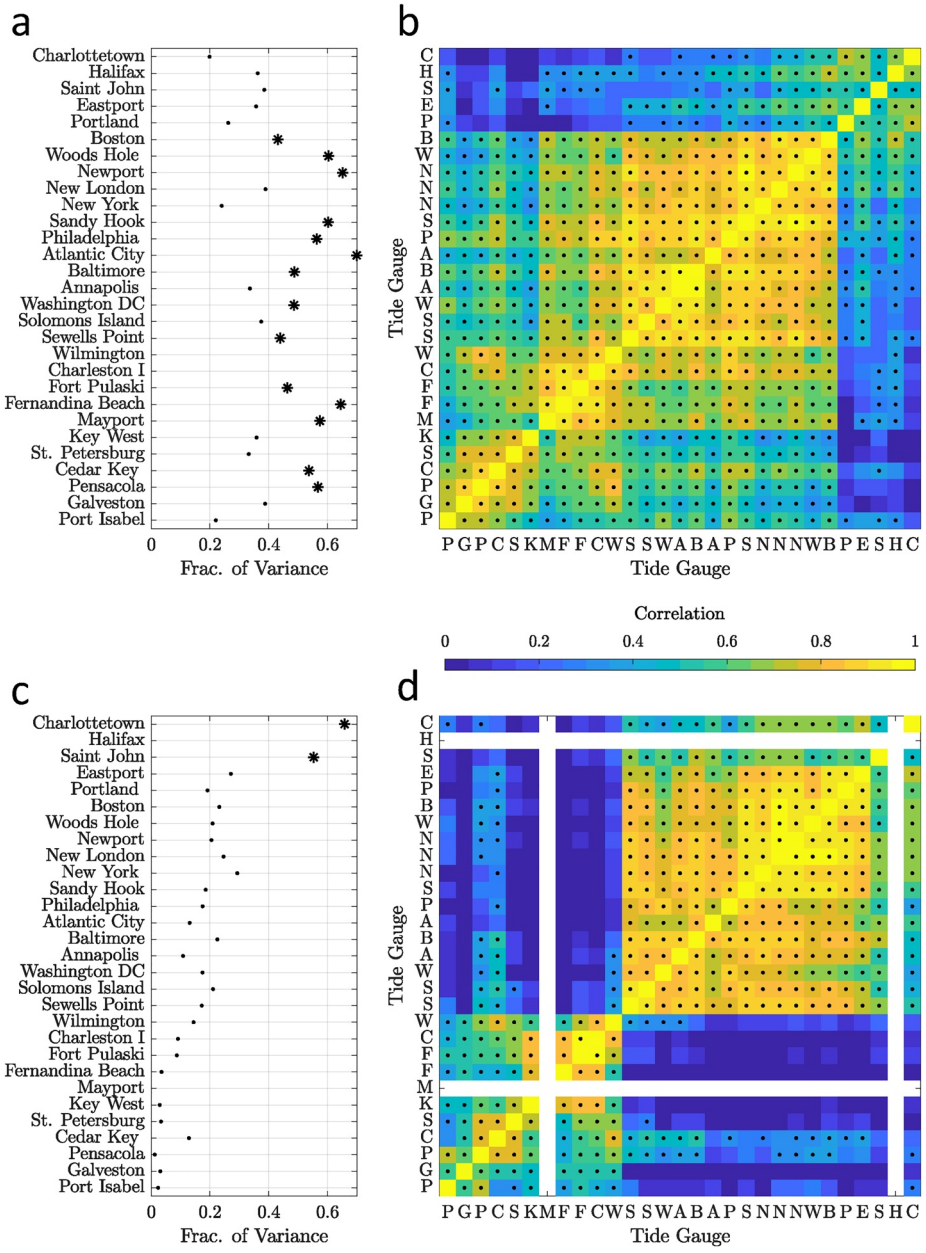

Figure 3. (a, c) Fraction of the total ζ variance within the 10–15 years frequency band over the (a) 1959–1988 and (c) 1989–2018 epoch. Tide gauges that are significant at the $p < 0.1$ level are shown with asterisks. (b, d) Cross-correlation of ζ between pairs of tide gauges over the (b) 1959–1988 and (d) 1989–2018 epoch. Significance at the $p < 0.1$ level is shown with stippling.

Figures S3–S5 suggest that power in the decadal band comprises a substantial fraction of the total variance. Indeed, this band comprises anywhere between 10% and 50% of the overall ζ variance over the entire record, although this fractional variance varies in time (Figures 3a and 3c). The large and time-varying contribution of decadal variability, in turn, implies that its spatial coherence (i.e., Figure 2c) will meaningfully impact along coast correlations.

In Figures 3b and 3d, we calculate cross-correlations over two different continuous 30-year epochs over which most tide gauges have annual mean values. When along coast coherence in the decadal band is relatively high (1959–1988; Figure 3b), the drop in correlation across Cape Hatteras emphasized in previous

studies is far more muted than when compared with the complete record. Instead, a break in correlation occurs south of the Gulf of Maine, between Boston and Portland, Maine. In contrast, cross-correlation for tide gauges on either side of Cape Hatteras is very low during a 30-year epoch of low coherence in the decadal band (1989–2018; Figure 3d).

Thus, while there remains the potential for multidecadal variation in alongshore coherence in other frequency bands, we find a clear temporal dependence in cross-correlation in the direction expected from analysis of the decadal band.

4. Discussion and Conclusions

Using tide gauges along the North American east coast, we find strong evidence for multidecadal epochs of enhanced decadal sea-level variability, with a time-varying along coast spatial expression. Our results help reconcile studies that emphasize the presence of both correlated (Thompson & Mitchum, 2014) and uncorrelated (Piecuch et al., 2017) sea-level variability across Cape Hatteras. The key insights provided here are that (a) variability in the decadal frequency band is responsible for much of the observed spatial structure; and (b) measures of along coast coherence are sensitive to the time period analyzed.

The epoch of measurements considered in different studies may thus contribute to their interpretation. For example, Thompson and Mitchum (2014) emphasize along coast coherence in their analysis of the 1952–2009 period, which encompasses the time period of high coherence in the decadal band (1960–1990; Figure 2). Similarly, Thompson (1986) finds coherence across Cape Hatteras at longer than interannual timescales over the 1950–1975 period. In contrast, Piecuch et al. (2017) consider 1980–2010 and emphasize a lack of coherence across Cape Hatteras.

Perhaps more important than the specific time period analyzed is a reliance on cross-correlation analyses, which blend spatial structures associated with different frequency bands and epochs. Although we have not considered spatial structure outside decadal periods, our results suggest that frequency-dependent characterization, or filtering, of tide gauge records will be more informative of the physical processes underlying spatial covariance. The frequency-dependent and time-dependent spatial structure of coastal sea-level variability also suggest caution in (a) the interpretation of stationary tide gauge indices as measures of climate and/or ocean circulation variability (e.g., Ezer, 2015; McCarthy et al., 2015; Valle-Levinson et al., 2017) and (b) the robustness of covariance assumptions used to fill spatial and temporal gaps in sea-level reconstructions (Kopp, 2013; Piecuch, Huybers, et al., 2018). In addition, it is worth considering the representativeness of the Key West tide gauge: although of particular importance because of the length of its record (e.g., Woodworth et al., 2017), it exhibits less variability at decadal timescales than tide gauges in either along coast direction. Tide gauges in Pensacola (e.g., Thompson et al., 2016) and Portland, Maine (e.g., Miller & Douglas, 2007) have also been interpreted in terms of much larger-scale variability.

Although identifying the physical processes underlying decadal east coast sea-level variability is beyond the scope of this paper, we note that earlier studies of sea surface temperature (SST) in the North Atlantic have highlighted enhanced (but not time-dependent) power in this frequency band (Czaja & Marshall, 2001; Wu & Liu, 2005), with Wu and Liu (2005) explicitly identifying high decadal power in the North Atlantic SST tripole. The NAO, in contrast, does not show enhanced power in this frequency band (e.g., Hurrell et al., 2003), supporting studies suggesting that ocean dynamics drive SST anomalies over decadal and longer timescales (e.g., Paeth et al., 2003). Over shorter (interannual) periods, the SST tripole has been found to be strongly correlated with North Atlantic sea surface height (an "SSH tripole," with out-of-phase coastal sea level variability across Cape Hatteras) (Volkov et al., 2019). Investigations of the relationship between the SST and SSH tripoles and ocean dynamics at decadal timescales, including those governing Gulf Stream variability (e.g., Ezer, 2019; Ezer & Dangendorf, 2020; Hameed et al., 2018; Nigam et al., 2018), are likely to be informative.

To our knowledge, modulation of power within this frequency band has not been described, in the context of SSTs or sea level. Plausible explanations for modulation include a change in the background climate state through secular or multidecadal variability (e.g., AMV; Zhang et al., 2019), or interference by two periodic signals with similar frequencies. Changes in the background state might include both atmospheric

(a change in the NAO center of action associated with shifts in the SST tripole, or AMV) and/or oceanic processes (changes in stratification or shifts in Gulf Stream position). If such modulation is related to AMV, it raises the possibility that the effect of AMOC strength variations on coastal sea level is predominantly through modulation of decadal variability, rather than through large-scale coincident changes in mean sea level (as considered in, e.g., Little et al., 2019). With respect to the possibility that modulation is driven by interfering, periodic signals, superimposed variability at 11 and 13.8 year periods would "beat" at 55 year periods with an apparent frequency of 12.4 years, roughly consistent with Figure 2. The responsible processes underlying periodicity at these frequencies are not clear, although the former period is similar to the solar cycle (Valle-Levinson & Martin, 2020) and the latter has been identified in the Arctic Oscillation index (Jevrejeva et al., 2003). A key difficulty for assessment of this possibility is the inability to observe multiple modulation cycles at most locations and resolve closely spaced spectral peaks. However, we note that ζ at the Battery tide gauge (Figure 1c) appears to show enhanced variability before ~1930, although at a slightly longer period than enhanced decadal variability observed after ~1980. More definitive statements regarding the origin of enhanced decadal sea-level variability are limited by the length of east coast tide gauge records. Extended sea level time series available through archival records (Hogarth, 2014; Talke et al., 2018), high-resolution proxies (e.g., Kemp et al., 2015), or long integrations of ocean and/or climate models (e.g., Kageyama et al., 2017), are potentially valuable for the characterization of centennial-timescale modulation, although model and proxy representation errors must be considered carefully.

Finally, returning to implications for sea-level "hotspots," we note that the amplitude of decadal east coast sea-level variability is relatively large (up to ~10 cm), and that multidecadal changes in its amplitude are sufficient to drive long periods of enhanced and/or muted coastal flooding. Although the decadal variability analyzed in this paper may not fully capture all aspects of sea-level variability that have been subsumed into the term "hotspots," it comprises a substantial fraction of the annual mean sea-level variance. Understanding the relevant underlying processes, and their predictability, may thus enhance the ability to quantify future coastal flood risk.

Data Availability Statement

Tide gauge data are freely available from the Permanent Service for Mean Sea Level (http://www.psmsl.org/data/obtaining/).

Acknowledgments
Christopher M. Little acknowledges funding support from NSF Grant OCE-1805029. CGP and RMP were funded through NASA Sea Level Change Team (CGP: Grant 80NSSC20K1241). The authors thank the developers of the freely available cross-wavelet and wavelet coherence toolbox for MATLAB.

References

Boon, J. D. (2012). Evidence of sea level acceleration at U.S. and Canadian tide stations, Atlantic Coast, North America. *Journal of Coastal Research*, *285*, 1437–1445. https://doi.org/10.2112/JCOASTRES-D-12-00102.1

Czaja, A., & Marshall, J. (2001). Observations of atmosphere-ocean coupling in the North Atlantic. *Quarterly Journal of the Royal Meteorological Society*, *127*(576), 1893–1916. https://doi.org/10.1002/qj.49712757603

Domingues, R., Goni, G., Baringer, M., & Volkov, D. (2018). What caused the accelerated sea level changes along the U.S. East Coast during 2010-2015? *Geophysical Research Letters*, *45*, 13367–13376. https://doi.org/10.1029/2018GL081183

Ezer, T. (2015). Detecting changes in the transport of the Gulf Stream and the Atlantic overturning circulation from coastal sea level data: The extreme decline in 2009–2010 and estimated variations for 1935–2012. *Global and Planetary Change*, *129*, 23–36. https://doi.org/10.1016/j.gloplacha.2015.03.002

Ezer, T. (2019). Regional differences in sea level rise between the mid-Atlantic Bight and the South Atlantic Bight: Is the Gulf Stream to Blame? *Earth's Future*, *7*(7), 771–783. https://doi.org/10.1029/2019EF001174

Ezer, T., & Atkinson, L. P. (2014). Accelerated flooding along the U.S. East Coast: On the impact of sea-level rise, tides, storms, the Gulf Stream, and the North Atlantic Oscillations. *Earth's Future*, *2*(8), 362–382. https://doi.org/10.1002/2014EF000252

Ezer, T., & Dangendorf, S. (2020). Global sea level reconstruction for 1900–2015 reveals regional variability in ocean dynamics and an unprecedented long weakening in the Gulf Stream flow since the 1990s. *Ocean Science*, *16*(4), 997–1016. https://doi.org/10.5194/os-16-997-2020

Goddard, P. B., Yin, J., Griffies, S. M., & Zhang, S. (2015). An extreme event of sea-level rise along the Northeast coast of North America in 2009–2010. *Nature Communications*, *6*(1). https://doi.org/10.1038/ncomms7346

Grinsted, A., Moore, J. C., & Jevrejeva, S. (2004). Application of the cross wavelet transform and wavelet coherence to geophysical time series.

Hameed, S., Wolfe, C. L. P., & Chi, L. (2018). Impact of the Atlantic meridional mode on Gulf Stream North Wall position. *Journal of Climate*, *31*(21), 8875–8894. https://doi.org/10.1175/JCLI-D-18-0098.1

Hamlington, B. D., Leben, R. R., Kim, K.-Y., Nerem, R. S., Atkinson, L. P., & Thompson, P. R. (2015). The effect of the El Niño-Southern Oscillation on U.S. regional and coastal sea level. *Journal of Geophysical Research: Oceans*, *120*(6), 3970–3986. https://doi.org/10.1002/2014JC010602

Hogarth, P. (2014). Preliminary analysis of acceleration of sea level rise through the twentieth century using extended tide gauge data sets. *Journal of Geophysical Research: Oceans*, *119*(11), 7645–7659. https://doi.org/10.1002/2014JC009976

Holgate, S. J., Matthews, A., Woodworth, P. L., Rickards, L. J., Tamisiea, M. E., Bradshaw, E., & Pugh, J. (2013). New data systems and products at the permanent service for mean sea level. *Journal of Coastal Research*, *29*(3), 493–504.

Hurrell, J. W., Kushnir, Y., Ottersen, G., & Visbeck, M. (2003). An overview of the North Atlantic Oscillation. In *The North Atlantic Oscillation: Climatic significance and environmental impact* (pp. 1–35). American Geophysical Union. Retrieved from. https://agupubs.onlinelibrary.wiley.com/doi/abs/10.1029/134GM01

Jevrejeva, S., Moore, J. C., & Grinsted, A. (2003). Influence of the Arctic Oscillation and El Niño-Southern Oscillation (ENSO) on ice conditions in the Baltic Sea: The wavelet approach. *Journal of Geophysical Research*, *108*(D21). 4677. https://doi.org/10.1029/2003JD003417

Kageyama, M., Albani, S., Braconnot, P., Harrison, S. P., Hopcroft, P. O., Ivanovic, R. F., et al. (2017). The PMIP4 contribution to CMIP6 – Part 4: Scientific objectives and experimental design of the PMIP4-CMIP6 last glacial maximum experiments and PMIP4 sensitivity experiments. *Geoscientific Model Development*, *10*(11), 4035–4055. https://doi.org/10.5194/gmd-10-4035-2017

Kemp, A. C., Hawkes, A. D., Donnelly, J. P., Vane, C. H., Horton, B. P., Hill, T. D., et al. (2015). Relative sea-level change in Connecticut (USA) during the last 2200 yrs. *Earth and Planetary Science Letters*, *428*, 217–229. https://doi.org/10.1016/j.epsl.2015.07.034

Kenigson, J. S., Han, W., Rajagopalan, B., Yanto, & Jasinski, M. (2018). Decadal shift of NAO-linked interannual sea level variability along the U.S. Northeast Coast. *Journal of Climate*, *31*(13), 4981–4989. https://doi.org/10.1175/JCLI-D-17-0403.1

Kopp, R. E. (2013). Does the mid-Atlantic United States sea level acceleration hot spot reflect ocean dynamic variability?: Sea level acceleration hot spot. *Geophysical Research Letters*, *40*(15), 3981–3985. https://doi.org/10.1002/grl.50781

Little, C. M., Hu, A., Hughes, C. W., McCarthy, G. D., Piecuch, C. G., Ponte, R. M., & Thomas, M. D. (2019). The relationship between United States East Coast sea level and the Atlantic Meridional Overturning Circulation: A review. *Journal of Geophysical Research: Oceans*, *124*, 6435–6458. https://doi.org/10.1029/2019JC015152

McCarthy, G. D., Haigh, I. D., Hirschi, J. J.-M., Grist, J. P., & Smeed, D. A. (2015). Ocean impact on decadal Atlantic climate variability revealed by sea-level observations. *Nature*, *521*(7553), 508–510. https://doi.org/10.1038/nature14491

Meade, R. H., & Emery, K. O. (1971). Sea level as affected by River Runoff, Eastern United States. *Science, New Series*, *173*(3995), 425–428. https://doi.org/10.1126/science.173.3995.425

Menéndez, M., & Woodworth, P. L. (2010). Changes in extreme high water levels based on a quasi-global tide-gauge data set. *Journal of Geophysical Research*, *115*(C10), C10011. https://doi.org/10.1029/2009JC005997

Miller, L., & Douglas, B. C. (2007). Gyre-scale atmospheric pressure variations and their relation to 19th and 20th century sea level rise. *Geophysical Research Letters*, *34*(16). L16602. https://doi.org/10.1029/2007GL030862

Nicholls, R. J., & Cazenave, A. (2010). Sea-level rise and its impact on coastal zones. *Science*, *328*(5985), 1517–1520. https://doi.org/10.1126/science.1185782

Nigam, S., Ruiz-Barradas, A., & Chafik, L. (2018). Gulf stream excursions and sectional detachments generate the decadal pulses in the Atlantic Multidecadal Oscillation. *Journal of Climate*, *31*(7), 2853–2870. https://doi.org/10.1175/JCLI-D-17-0010.1

Paeth, H., Latif, M., & Hense, A. (2003). Global SST influence on twentieth century NAO variability. *Climate Dynamics*, *21*(1), 63–75. https://doi.org/10.1007/s00382-003-0318-4

Piecuch, C. G., Bittermann, K., Kemp, A. C., Ponte, R. M., Little, C. M., Engelhart, S. E., & Lentz, S. J. (2018). River-discharge effects on United States Atlantic and Gulf coast sea-level changes. *Proceedings of the National Academy of Sciences of the United States of America*, *115*(30), 7729–7734. https://doi.org/10.1073/pnas.1805428115

Piecuch, C. G., Dangendorf, S., Ponte, R. M., & Marcos, M. (2017). Annual sea level changes on the North American Northeast Coast: Influence of local winds and barotropic motions. *Journal of Climate*, *29*(13), 4801–4816. https://doi.org/10.1175/jcli-d-16-0048.1

Piecuch, C. G., Huybers, P., Hay, C. C., Kemp, A. C., Little, C. M., Mitrovica, J. X., et al. (2018). Origin of spatial variation in US East Coast sea-level trends during 1900–2017. *Nature*, *564*(7736), 400–404. https://doi.org/10.1038/s41586-018-0787-6

Piecuch, C. G., Huybers, P., & Tingley, M. P. (2017). Comparison of full and empirical Bayes approaches for inferring sea-level changes from tide-gauge data. *Journal of Geophysical Research: Oceans*, *122*(3), 2243–2258. https://doi.org/10.1002/2016JC012506

Sallenger, A. H., Doran, K. S., & Howd, P. A. (2012). Hotspot of accelerated sea-level rise on the Atlantic coast of North America. *Nature Climate Change*, *2*(12), 884–888. https://doi.org/10.1038/nclimate1597

Sweet, W. V., Menendez, M., Genz, A., Obeysekera, J., Park, J., & Marra, J. J. (2016). Tide's way: Southeast Florida's September 2015 Sunny-day Flood. *Bulletin of the American Meteorological Society*, *97*, S25–S30. https://doi.org/10.1175/BAMS-D-16-0117.1

Talke, S. A., Kemp, A. C., & Woodruff, J. (2018). Relative sea level, tides, and extreme water levels in Boston Harbor from 1825 to 2018. *Journal of Geophysical Research: Oceans*, *123*(6), 3895–3914. https://doi.org/10.1029/2017JC013645

Thompson, K. R. (1986). North Atlantic sea-level and circulation. *Geophysical Journal International*, *87*(1), 15–32. https://doi.org/10.1111/j.1365-246X.1986.tb04543.x

Thompson, P. R., Hamlington, B. D., Landerer, F. W., & Adhikari, S. (2016). Are long tide gauge records in the wrong place to measure global mean sea level rise?: Global mean sea level from tide gauges. *Geophysical Research Letters*, *43*(19), 10403–10411. https://doi.org/10.1002/2016GL070552

Thompson, P. R., & Mitchum, G. T. (2014). Coherent sea level variability on the North Atlantic western boundary. *Journal of Geophysical Research: Oceans*, *119*(9), 5676–5689. https://doi.org/10.1002/2014JC009999

Torrence, C., & Webster, P. J. (1999). Interdecadal changes in the ENSO–Monsoon system. *Journal of Climate*, *12*(8). https://doi.org/10.1175/1520-0442(1999)012<2679:icitem>2.0.co;2

Valle-Levinson, A., Dutton, A., & Martin, J. B. (2017). Spatial and temporal variability of sea level rise hot spots over the eastern United States: Sea level rise hot spots over Eastern U.S. *Geophysical Research Letters*, *44*(15), 7876–7882. https://doi.org/10.1002/2017GL073926

Valle-Levinson, A., & Martin, J. B. (2020). Solar activity and lunar precessions influence extreme sea-level variability in the U.S. Atlantic and Gulf of Mexico Coasts. *Geophysical Research Letters*, *47*(20). e2020GL090024. https://doi.org/10.1029/2020GL090024

Volkov, D. L., Lee, S.-K., Domingues, R., Zhang, H., & Goes, M. (2019). Interannual sea level variability along the southeastern seaboard of the United States in relation to whom it may concern: The gyre-scale heat divergence in the North Atlantic. *Geophysical Research Letters*, *46*(13), 7481–7490. https://doi.org/10.1029/2019GL083596

Woodworth, P. L., Maqueda, M. Á. M., Gehrels, W. R., Roussenov, V. M., Williams, R. G., & Hughes, C. W. (2017). Variations in the difference between mean sea level measured either side of Cape Hatteras and their relation to the North Atlantic Oscillation. *Climate Dynamics*, *49*(7–8), 2451–2469. https://doi.org/10.1007/s00382-016-3464-1

Woodworth, P. L., Maqueda, M. Á. M., Roussenov, V. M., Williams, R. G., & Hughes, C. W. (2014). Mean sea-level variability along the northeast American Atlantic coast and the roles of the wind and the overturning circulation. *Journal of Geophysical Research: Oceans*, *119*(12), 8916–8935. https://doi.org/10.1002/2014JC010520

Wu, L., & Liu, Z. (2005). North Atlantic decadal variability: Air–sea coupling, oceanic memory, and potential Northern Hemisphere Resonance*. *Journal of Climate*, *18*(2), 331–349. https://doi.org/10.1175/JCLI-3264.1

Yin, J., & Goddard, P. B. (2013). Oceanic control of sea level rise patterns along the East Coast of the United States. *Geophysical Research Letters*, *40*(20), 5514–5520. https://doi.org/10.1002/2013GL057992

Zhang, R., Sutton, R., Danabasoglu, G., Kwon, Y.-O., Marsh, R., Yeager, S. G., et al. (2019). A review of the role of the Atlantic meridional overturning circulation in Atlantic multidecadal variability and associated climate impacts. *Reviews of Geophysics*, *57*(2), 316–375. https://doi.org/10.1029/2019rg000644